hv photonics

IMPACT FACTOR 2.1

CITESCORE 2.6

Article

A Fast Rearrangement Method for Defect-Free Atom Arrays

Yuqing Zhang, Zeyan Zhang, Guoqing Zhang, Zhehua Zhang, Yanpu Chen, Yuqing Li, Wenliang Liu, Jizhou Wu, Vladimir Sovkov and Jie Ma

MDPI

https://doi.org/10.3390/photonics12020117

photonics

MDPI

Article

A Fast Rearrangement Method for Defect-Free Atom Arrays

Yuqing Zhang [1], Zeyan Zhang [1], Guoqing Zhang [1], Zhehua Zhang [1], Yanpu Chen [1], Yuqing Li [1,2], Wenliang Liu [1,2], Jizhou Wu [1,2,*], Vladimir Sovkov [1,3] and Jie Ma [1,2]

[1] State Key Laboratory of Quantum Optics Technologies and Devices, Shanxi University, Taiyuan 030006, China; 202222618053@email.sxu.edu.cn (Y.Z.); 202422603017@email.sxu.edu.cn (Z.Z.); 202312603026@email.sxu.edu.cn (G.Z.); 202412603032@email.sxu.edu.cn (Z.Z.); 202412603001@email.sxu.edu.cn (Y.C.); lyqing2006@sxu.edu.cn (Y.L.); liuwl@sxu.edu.cn (W.L.); vladimir_sovkov@mail.ru (V.S.); mj@sxu.edu.cn (J.M.)
[2] Collaborative Innovation Center of Extreme Optics, Shanxi University, Taiyuan 030006, China
[3] Department of Photonics, St. Petersburg State University, 7/9 Universitetskaya Nab., 199034 St. Petersburg, Russia
* Correspondence: wujz@sxu.edu.cn

Abstract: Defect-free atom arrays provide new possibilities for exploring exotic quantum phenomena and realizing quantum computing. However, quickly and efficiently preparing defect-free atom arrays poses challenges. This paper proposes an innovative parallel rearrangement method, namely the parallel compression filling algorithm (PCFA), wherein multiple movable optical tweezers operate simultaneously. By limiting the shape of the initial loading, the method reduces movement complexity. The simulation comparisons show that this algorithm is more efficient in preparing defect-free atom arrays and can also be applied to the generation of other periodic structure arrays. The simulation results show that, in most cases, preparing a defect-free array of 400 atoms requires no more than 30 steps.

Keywords: atom array; optical tweezer; rearrangement

Received: 12 December 2024
Revised: 11 January 2025
Accepted: 27 January 2025
Published: 28 January 2025

Citation: Zhang, Y.; Zhang, Z.; Zhang, G.; Zhang, Z.; Chen, Y.; Li, Y.; Liu, W.; Wu, J.; Sovkov, V.; Ma, J. A Fast Rearrangement Method for Defect-Free Atom Arrays. *Photonics* **2025**, *12*, 117. https://doi.org/10.3390/photonics12020117

1. Introduction

Neutral atom array platforms demonstrate significant potential for large-scale quantum computing due to their scalability and programmability [1–7]. Through leveraging the strong interactions between Rydberg atoms, scientists can perform efficient quantum logic operations and simulate complex physical systems. This platform is not only suitable for quantum information processing [8–14] but is also widely applied in topological physics [15–17], many-body dynamics [18–22], and quantum precision measurement [23–25] research.

The generation of defect-free atom arrays is crucial for these applications. However, due to collisional blockade effects, the initial loading rate of optical tweezer arrays is typically only 50% [26,27]. The use of acousto-optic deflectors (AODs) effectively addresses this challenge. The establishment of dynamic optical tweezers with AODs enables the movement of incorrectly positioned atoms to their target locations based on the positional information of the initially loaded atoms. This process follows specific algorithms, resulting in the creation of defect-free atom arrays. The lifetime of atoms in optical tweezers is limited, particularly for large-scale atomic arrays, where atomic lifetime decreases with an increase in the number of atoms. Therefore, it is particularly important to develop efficient rearrangement algorithms. Previous research primarily focused on the manipulation of individual atoms, usually sorting atoms individually using techniques such as heuristic clustering algorithms (HCAs) [28], compression algorithms, and linear sum assignment

problems (LSAPs) [29]. However, mutual blockade during the movement of single atoms restricts the number of moves in a linear relation to the size of the target array, even after optimization.

This paper presents a novel parallel rearrangement method that integrates spatial light modulator (SLM) configurations with a parallel rearrangement algorithm. In this method, atoms move only within the same row or column during rearrangement, independently of atoms in other rows or columns. The method employs a computer simulation analysis to assess the efficacy of this approach in reducing rearrangement steps and compares it with existing algorithms, demonstrating its advantages in enhancing rearrangement efficiency. In addition, the experiment system used to implement the algorithm and the concrete steps is also presented.

2. Rearrangement Method

Recent reports have demonstrated the parallel movements and even the overall movements of the entire array [11,22,30], showcasing enhanced control capabilities for optical tweezers in terms of efficiency and precision. Based on this, we propose a more efficient approach for preparing defect-free atom arrays. We imposed restrictions on the configuration of the SLM target light field. To construct a defect-free atom array in the shape of a square, the target light field is configured as a rectangular optical tweezers array, with the number of tweezers along the longer side slightly greater than that on the shorter side, divided by the initial loading rate. For example, the target light field of the SLM should be set to an 8×18 rectangular optical tweezers array in order to prepare a defect-free atom array consisting of 64 atoms with an initial loading rate of 50%. This setup aims to maximize the number of atoms that are initially loaded in each row at the current loading rate. The reorganization strategy, namely the parallel compression filling algorithm (PCFA), includes two stages: row compression and filling defective rows.

The row compression process is performed on a row-by-row basis, following the principle of arranging the randomly filled atoms within the array to form a defect-free atom chain. Due to our restrictions on the diffracted light field of the SLM, most rows contain more atoms than the target number. Therefore, only a small amount of additional filling is required in the second step to complete the rearrangement of the defect-free atom array. During this filling process, we select atoms from the row with the maximum number of atoms to fill up rows that do not have a maximal number of atoms, thus minimizing any unnecessary movements.

3. Algorithm Details

We demonstrate the process of rearranging a 6×6 defect-free atom array to prove the feasibility of our algorithm. Assuming an initial filling rate of 50%, as described above, the first step is to construct a rectangular optical tweezers array with dimensions of 6×14 using the SLM. The process of rearrangement in a trial computer simulation is illustrated in Figure 1.

(1) Initial state: After randomly filling the atoms, the atomic occupancy situation is determined via capturing fluorescence images using an electron-multiplying charge-coupled device (EMCCD). Firstly, the total number of atoms is assessed to determine whether it exceeds the required number for the target array. If this condition is not met, reloading and reassessment are repeated until the total number of loaded atoms meets or exceeds the required number.

(2) Row compression: This step involves calculating the necessary waveforms by considering the atomic positions and summing the corresponding waveforms of atoms in each row, followed by arranging them sequentially. It is crucial to note that an initial phase

processing is required during waveform calculation to suppress the frequency intermodulation effects. If executed with maximum parallelism, only L steps are needed, where L is the number of atoms on one side of the target square array.

(3) Fill the gap: After compression, some rows contain fewer atoms than L, necessitating that these are filled with extra atoms from other rows. The filling process is also carried out in parallel. When there are multiple gaps, the selection of which rows to fill directly affects the overall efficiency of the reorganization procedure. To minimize unnecessary movements, we prioritize utilizing atoms from the rows with the most atoms to fill the rows that exhibit the most of gaps, aiming to complete the filling in a single move. If any gaps remain after the shorter rows have been filled, this process is repeated until all rows have been filled.

(4) Eject excess atoms: All the excess atoms are located on one side of the array. We can efficiently remove these excess atoms in a single step by generating a moving optical tweezers array that covers the atoms and moves them beyond the range of the static optical tweezers. This process ensures the successful preparation of a defect-free atom array.

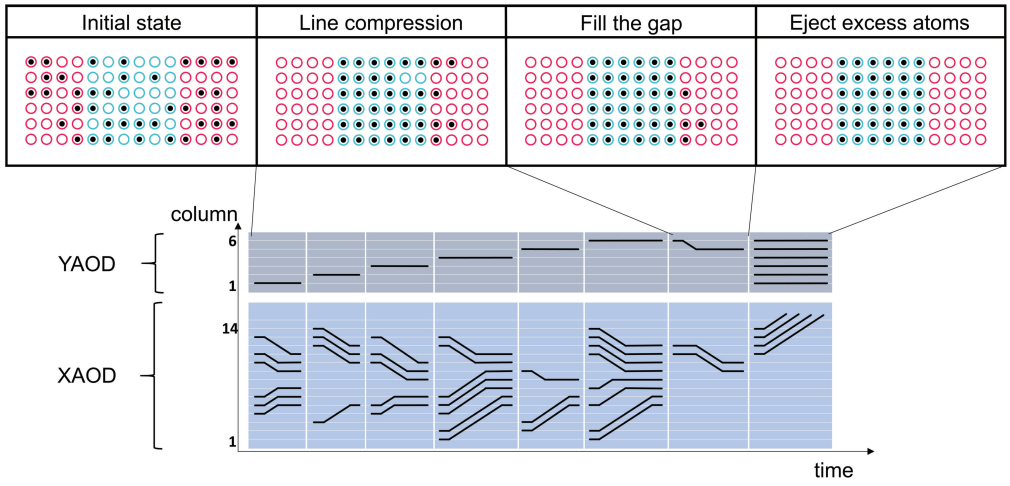

Figure 1. Example of the rearrangement process: The upper panel illustrates the reconfiguration steps; the circles represent the optical tweezers; the black dots represent the atoms; the blue and red background area denotes the target sites and reservoir, respectively; the lower panel shows the frequency spectrum of the vertical and horizontal AOD waveforms corresponding to each reconfiguration step.

It is worth noting that, although we have only demonstrated the preparation process for a square defect-free array, this reorganization method is also applicable to other periodic target arrays, such as staggered, Kagome, and honeycomb lattices [31–33]. The SLM configurations are shown in Figure 2.

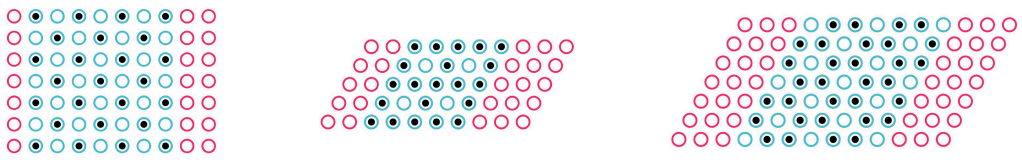

(a) Staggered (b) Kagome (c) Honeycomb

Figure 2. Examples of periodic staggered (**a**), Kagome (**b**), and honeycomb (**c**) lattice structures. The blue area represents the target structure, while the red area indicates the reservoirs that require additional configuration when using PCFA.

4. Comparison with Existing Algorithms

In traditional single-tweezers reorganization, a single move can, at most, fill one vacancy and, if there are atoms blocking the path, additional steps will be needed. In the previously developed single-tweezers moving algorithms, the compression algorithm has a relatively high reorganization efficiency. To demonstrate the superiority of our proposed method in terms of movement efficiency, we compared the movement efficiency of our method with the compression algorithm at different array scales. In the computer simulation, the initial loading rate was set to 50%, and the target array was a $N = L \times L$ defect-free square array. Using the maximum parallelism, we took the average of multiple simulations. As shown in Figure 3a, as the target array increased, the average number of moves of the compression algorithm increased linearly with N, but there was still a gap, stopping it from reaching the limit of $N/2$. However, the number of moves was far less than this limit in our scheme.

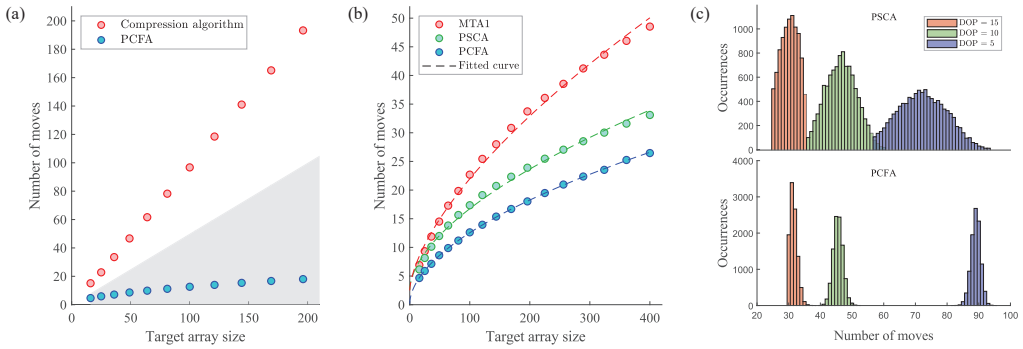

Figure 3. Algorithm comparison: (**a**) The number of moves required to rearrange defect-free atom arrays of different sizes using a compression algorithm (red circles) and the PCFA (blue circles). The shaded sections represent the limitations in the movement of the single optical tweezers at the current setting of the initial loading rate [29]; (**b**) A comparison of the number of moves required to rearrange defect-free atom arrays of different sizes using MTA1 (red circles), PSCA (green circles), and PCFA (blue circles); (**c**) Simulated distribution of moved numbers when rearranging 15 × 15 defected atomic arrays with a different DOP using the PSCA and PCFA.

Parallel rearrangement algorithms such as MTA1 and PSCA have been shown [22,30]. Unlike our method, both MTA1 and PSCA decompose the two-dimensional problem into several one-dimensional problems, transforming it into independent reorganizations of rows and columns. The process of both algorithms involves an initial stage of sorting rows to ensure that each column contains the required number of atoms for the target array, followed by a subsequent step of reorganizing the columns to complete the preparation of the target array. However, it should be noted that there are differences in terms of pre-sorting judgment and column reorganization steps between these two algorithms, which directly determine their efficiency in reorganization.

To compare their reorganization efficiency, we simulated and compared the number of moves of our proposed method with that of MTA1 and PSCA at different target array sizes. The initial loading rate was set to 55%, and the target arrays were the same as in Ref. [5], using the maximum parallelism. It is worth noting that we chose 55% because, for parallel rearrangement, increasing the initial load rate has no significant effect on the rearrangement efficiency. In PCFA, for example, even if the increase in the load rate makes the atom distribution more clustered, it is still necessary to traverse each row of rearrangement atoms to construct the target array. Therefore, we chose the same initial fill rate as in the reference. As shown in Figure 3b, the average number of moves for MTA1 is $N^{0.64}$, for PSCA is $N^{0.57}$, while the number of moves for our method is only $N^{0.54}$. Compared to MTA1 and PSCA, PFCA demonstrates superior rearrangement efficiency.

This is primarily attributed to its ability to effectively simplify the two-dimensional array rearrangement into a nearly one-dimensional process. By elongating the SLM optical tweezer array along one dimension and increasing the number of loaded atoms per row, we could ensure that the average number of atoms per row at the current filling rate remained over L. This means that, in some possible loading processes, each row has no less than L atoms, allowing for the reorganization to be completed in no more than L steps with maximum parallelism. Even if there are vacancies, there is a clear choice for filing them after compression. In contrast, the pre-sorting stage necessitates scanning and adjusting the distribution of atoms, inevitably leading to the creation and subsequent filling of vacancies as an intermediate process. By employing the method proposed in this paper, it typically takes less than 30 steps to prepare a 20×20 defect-free atom array.

In the previous simulations, we used maximum parallelism. The PCFA also features an adjustable degree of parallelism (DOP), which denotes the maximum number of optical tweezers that can be operated simultaneously. For example, if DOP = 5, it would takes at least two steps to move eight atoms. Figure 3c shows the step distribution of a 15×15 defect-free atomic array completed with different DOPs. It is evident that increased parallelism enhances efficiency. When the DOP is large, the rearrangement efficiency of the PSCA and PCFA becomes comparable. The row compression stage of the PCFA requires traversing nearly the entire range of the optical tweezers array. Therefore, as the DOP decreases, the number of moves linearly increases, thereby diminishing the advantage of the PCFA compared to the PSCA.

In addition, a comparable parallel rearrangement technique, known as the post-selection method, is also introduced in references [10,34]. Similar to the PCFA, this method limits the SLM configuration to L rows. However, it introduces a post-selection evaluation after row compression. If defects are identified, the process will be abandoned and restarted until the target array is successfully completed. Undoubtedly, the post-selection method requires the fewest moves when rearranging with the same degree of parallelism. However, its discarding of defective cases increases the need for a larger reservoir to ensure a successful rearrangement rate. In contrast, under identical conditions regarding reservoir size, filling rate, and target array, the PCFA method exhibits a higher success rate for rearrangement. Moreover, the PCFA can construct a larger defect-free atom array within the constraints of an optical tweezers array configured using the SLM.

5. Experiment Preparation

The experimental validation of the method is under construction. The experimental setup is depicted in Figure 4a. The glass cell that housed the magneto-optical trap (MOT) section maintains a vacuum pressure of 10^{-12} mbar using an ion pump. The atomic cloud in the MOT was cooled to $\sim$20 µK after polarization gradient cooling. A static optical tweezer array was created by focusing laser light reflected from a spatial light modulator (LCOS-SLM, Hamamatsu) through a high numerical aperture (NA = 0.5) microscope objective. The hologram design utilized the weighted Gerchberg–Saxton (WGS) algorithm, which was further optimized with camera sampling feedback to homogenize the optical tweezer array, ensuring a relative standard deviation at a trap depth of less than 5%. This process achieved uniformity in the static optical tweezers, as depicted in Figure 4b,c.

The static optical tweezer array was focused at the center of the MOT for atom trapping; however, due to collision blockade effects, the initial loading rate was typically around 50%. To rearrange the randomly loaded atom array into a defect-free atom array, the system first uses an EMCCD to collect the fluorescence signals from the atoms in the static tweezers, obtaining their initial positions. This information is transmitted to a host computer, which calculates the rearrangement paths and the order for each atom based on specific algorithms.

The rearrangement process relies on the atomic position data derived from the images. Thus, our system can be regarded as a non-Markovian system [35,36], which significantly enhances the efficiency and reliability of atomic rearrangement by calculating the movement trajectories of atoms with a single feedback loop.

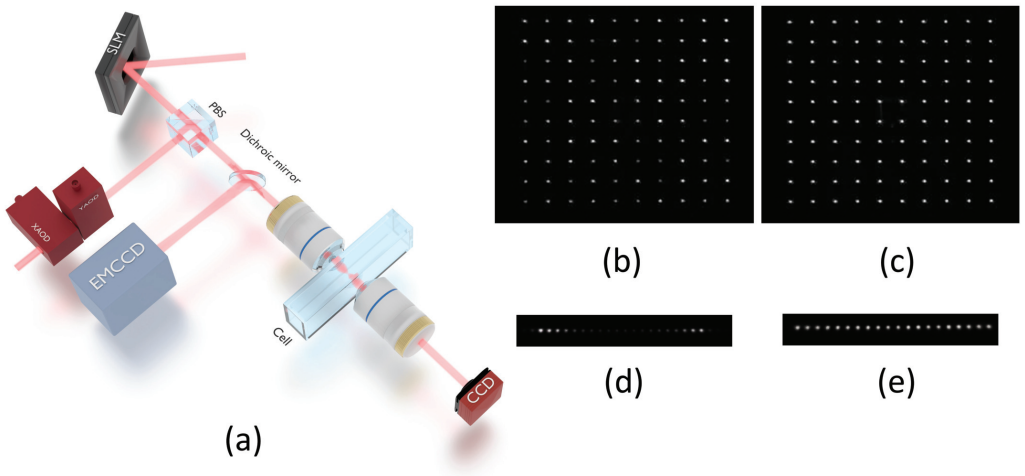

Figure 4. (**a**) Experimental setup: The diffracted light from the SLM and the 2D AOD is focused using a microscope objective (NA = 0.5), forming a static optical tweezer and a dynamic optical tweezer, respectively. These tweezers can be imaged onto a CCD camera using the same magnification for observation. The fluorescence from single atoms is collected by the objective after passing through a dichroic mirror, then it is imaged and analyzed by an EMCCD camera; (**b**,**c**) The static optical tweezer before and after homogenization, respectively; (**d**,**e**) The dynamic optical tweezer before and after homogenization, respectively.

Next, an arbitrary waveform generator (AWG, Spectrum Instrumentation) generates the corresponding waveform signals and sends them to a two-dimensional AOD (AA Opto Electronic).The laser light diffracted by the AOD is utilized to generate dynamic optical tweezers for precise control of atom movement. The relative positions of the two types of tweezers are measured using a CCD camera, and the operating frequency of the AOD is adjusted to align the positions of the dynamic tweezers with those of the static tweezers, ultimately achieving precise calibration between the AOD and SLM arrays.

The movement of atoms is accomplished through dynamic optical tweezers, involving three continuous steps: grabbing, moving, and releasing. To ensure that atoms are not heated during movement, these steps are executed without phase jumps. In the experiment, all waveforms for moving atoms from one optical trap to another are pre-calculated, and corresponding waveforms are selected based on the parallel rearrangement algorithm. By summing and assembling these waveforms, the resulting signal is output from the AWG to the AOD, facilitating atom movement.

However, when multiple control frequency signals are simultaneously applied to the AOD, nonlinear effects can lead to frequency intermodulation, resulting in reduced diffraction efficiency and an uneven distribution of intensity. This effect is particularly pronounced when the phases of these frequencies are highly correlated. To mitigate the impact of intermodulation effects, we homogenized the intensity of the diffracted light from the AOD prior to rearrangement. Specifically, we first randomized the initial phases of the multi-frequency signals [37], then adjusted the amplitude of the different frequency signals through CCD feedback, ultimately achieving a highly uniform intensity distribution in the array, as shown in Figure 4d,e.

The reflection loss of the objective leads to the insufficient use of the optical tweezers' light. Despite the commercial Ti:sapphire laser being capable of delivering more than 2 W

of continuous laser output, this limitation restricts the number of optical tweezer arrays to a few hundred.

6. Discussion and Conclusions

In this paper, we propose a PCFA method for the preparation of defect-free atom arrays. This method overcomes the limitations of traditional single-atom movement methods by dynamically controlling atom movement with parallel optical tweezers, achieving a more efficient and stable reorganization process. Our method is also applicable to most lattice shapes of interest, such as staggered, kagome, and honeycomb lattices. Additionally, the method is suitable for AOD static optical tweezers, with the only difference being that different lattices require the AOD to be rotated to a specific angle.

Similarly to other parallel algorithms, the PCFA enhances efficiency through the parallel control of atoms. However, the experimental parallel control capability of the optical tweezers is limited. Improving this capability can significantly enhance the efficiency of atomic rearrangement. Additionally, while the PCFA utilizes the SLM to construct more optical tweezers in one dimension, this approach may constrain the scalability of atomic arrays under the same conditions.

In summary, the reorganization method proposed in this paper provides a new approach and technical means for the efficient generation of defect-free atom arrays. It opens up new possibilities for exploring the broad applications of neutral atom arrays in quantum simulation, quantum computing, and other fields, further advancing the development of neutral atom array technology.

Author Contributions: Conceptualization, Y.Z. and J.W.; methodology, Y.Z.; software, Y.Z. and Z.Z. (Zeyan Zhang); validation, G.Z., Z.Z. (Zhehua Zhang), and Y.C.; resources, Y.L., W.L., J.W. and J.M.; data curation, Y.Z.; writing—original draft preparation, Y.Z.; writing—review and editing, J.W., V.S. and J.M.; visualization, Y.Z. and Z.Z. (Zeyan Zhang); supervision, J.W.; project administration, J.M.; funding acquisition, J.W. and J.M. All authors have read and agreed to the published version of the manuscript.

Funding: This work is supported by the Innovation Program for Quantum Science and Technology (Grant No. 2021ZD0302103), the National Natural Science Foundation of China (Grant Nos. 62325505, 62020106014, 62175140, 62475138) and the Shanxi Province Graduate Student Research Innovation Project (2024KY019, 2024JG018 and 2024TD03).

Institutional Review Board Statement: Not applicable.

Informed Consent Statement: Not applicable.

Data Availability Statement: The data included in this paper are not yet publicly available but can be obtained from the author upon reasonable request.

Conflicts of Interest: The authors declare no conflicts of interest.

References

1. Endres, M.; Bernien, H.; Keesling, A.; Levine, H.; Anschuetz, E.; Krajenbrink, A.; Senko, C.; Vuletic, V.; Greiner, M.; Lukin, M. Atom-by-atom assembly of defect-free one-dimensional cold atom arrays. *Science* **2016**, *354*, 1024–1027. [CrossRef]
2. Barredo, D.; De, L.S.; Lienhard, V.; Lahaye, T.;Browaeys, A. An atom-by-atom assembler of defect-free arbitrary two-dimensional atomic arrays. *Science* **2016**, *354*, 1021–1023. [CrossRef]
3. Barredo, D.; Lienhard, V.; De, L.S.; Lahaye, T.;Browaeys, A. Synthetic three-dimensional atomic structures assembled atom by atom. *Nature* **2018**, *561*, 79–82. [CrossRef]
4. Sheng, C.; Hou, J.; He, X.; Wang, K.;Guo, R.; Zhuang, J.; Mamat, B.; Xu, P.; Liu, M.; Wang, J.; et al. Defect-free arbitrary-geometry assembly of mixed-species atom arrays. *Phys. Rev. Lett.* **2022**, *128*, 083202. [CrossRef] [PubMed]

5. Liu, Y.; Wang, Z.; Yang, P.; Wang, Q.; Fan, Q.; Guan, S.; Li, G.; Zhang, P.; Zhang, T. Realization of strong coupling between deterministic single-atom arrays and a high-finesse miniature optical cavity. *Phys. Rev. Lett.* **2023**, *130*, 173601. [CrossRef] [PubMed]
6. Schymik, K.-N.; Ximenez, B.; Bloch, E.; Dreon, D.; Signoles, A.; Nogrette, F.; Barredo, D.; Browaeys, A.; Lahaye, T. In situ equalization of single-atom loading in large-scale optical tweezer arrays. *Phys. Rev. A* **2022**, *106*, 022611. [CrossRef]
7. Manetsch, H.J.; Nomura, G.; Bataille, E.; Leung, K.H.; Lv, X.; Endres, M. A tweezer array with 6100 highly coherent atomic qubits. *arXiv* **2024**, arXiv:2403.12021.
8. Evered, S.J.; Bluvstein, D.; Kalinowski, M.; Ebadi, S.; Manovitz, T.; Zhou, H.; Li, S.H.; Geim, A.A.; Wang, T.T.; Maskara, N.; et al. High-fidelity parallel entangling gates on a neutral-atom quantum computer. *Nature* **2023**, *622*, 268–272. [CrossRef]
9. Graham, T.; Song, Y.; Scott, J.; Poole, C.; Phuttitarn, L.; Jooya, K.; Eichler, P.; Jiang, X.; Marra, A.; Grinkemeyer, B.; et al. Multi-qubit entanglement and algorithms on a neutral-atom quantum computer. *Nature* **2022**, *604*, 457–462. [CrossRef]
10. Bluvstein, D.; Levine, H.; Semeghini, G.; Wang, T.T.; Ebadi, S.; Kalinowski, M.; Keesling, A.; Maskara, N.; Pichler, H.; Greiner, M.; et al. A quantum processor based on coherent transport of entangled atom arrays. *Nature* **2022**, *604*, 451–456. [CrossRef] [PubMed]
11. Bluvstein, D.; Evered, S.J.; Geim, A.A.; Li, S.H.; Zhou, H.; Manovitz, T.; Ebadi, S.; Cain, M.; Kalinowski, M.; Hangleiter, D.; et al. Logical quantum processor based on reconfigurable atom arrays. *Science* **2024**, *626*, 58–65. [CrossRef] [PubMed]
12. Picken, C.; Legaie, R.; McDonnell, K.; Pritchard, J. Entanglement of neutral-atom qubits with long ground-Rydberg coherence times. *Quantum Sci. Technol.* **2018**, *4*, 015011. [CrossRef]
13. Ebadi, S.; Keesling, A.; Cain, M.; Wang, T.T.; Levine, H.; Bluvstein, D.; Semeghini, G.; Omran, A.; Liu, J.; Samajdar, R.; et al. Quantum optimization of maximum independent set using Rydberg atom arrays. *Science* **2022**, *376*, 1209–1215. [CrossRef]
14. Llenas, A.; Lamata, L. Digital-analog quantum genetic algorithm using Rydberg-atom arrays. *Phys. Rev. A* **2024**, *110*, 042603. [CrossRef]
15. Chen, C.; Bornet, G.; Bintz, M.; Emperauger, G.; Leclerc, L.; Liu, V.S.; Scholl, P.; Barredo, D.; Hauschild, J.; Chatterjee, S.; et al. Continuous symmetry breaking in a two-dimensional Rydberg array. *Nature* **2023**, *616*, 691–695. [CrossRef] [PubMed]
16. De, L.S.; Lienhard, V.; Scholl, P.; Barredo, D.; Weber, S.; Lang, N.; Browaeys, A. Observation of a symmetry-protected topological phase of interacting bosons with Rydberg atoms. *Science* **2019**, *365*, 775–780.
17. Semeghini, G.; Levine, H.; Keesling, A.; Ebadi, S.; Wang, T.T.; Bluvstein, D.; Verresen, R.; Pichler, H.; Kalinowski, M.; Samajdar, R.; et al. Probing topological spin liquids on a programmable quantum simulator. *Science* **2021**, *374*, 1242–1247. [CrossRef] [PubMed]
18. Labuhn, H.; Barredo, D.; Ravets, S.; De Léséleuc, S.; Macrì, T.; Lahaye, T.; Browaeys, A. Tunable two-dimensional arrays of single Rydberg atoms for realizing quantum Ising models. *Nature* **2016**, *534*, 667–670. [CrossRef] [PubMed]
19. Zeiher, J.; Choi, J.Y.; Rubio-Abadal, A.; Pohl, T.; Van Bijnen, R.; Bloch, I.; Gross, C. Coherent many-body spin dynamics in a long-range interacting Ising chain. *Phys. Rev. X* **2017**, *7*, 041063. [CrossRef]
20. Bernien, H.; Schwartz, S.; Keesling, A.; Levine, H.; Omran, A.; Pichler, H.; Choi, S.; Zibrov, A.S.; Endres, M.; Greiner, M.; et al. Probing many-body dynamics on a 51-atom quantum simulator. *Nature* **2017**, *551*, 579–584. [CrossRef]
21. Browaeys, A.; Lahaye, T. Many-body physics with individually controlled Rydberg atoms. *Nat. Phys.* **2020**, 16, 132–142. [CrossRef]
22. Ebadi, S.; Wang, T.T.; Levine, H.; Keesling, A.; Semeghini, G.; Omran, A.; Bluvstein, D.; Samajdar, R.; Pichler, H.; Ho, W.W.; et al. Quantum phases of matter on a 256-atom programmable quantum simulator. *Nature* **2021**, *595*, 227–232. [CrossRef] [PubMed]
23. Bornet, G.; Emperauger, G.; Chen, C.; Ye, B.; Block, M.; Bintz, M.; Boyd, J.A.; Barredo, D.; Comparin, T.; Mezzacapo, F.; et al. Scalable spin squeezing in a dipolar Rydberg atom array. *Nature* **2023**, *621*, 728–733. [CrossRef]
24. Deist, E.; Gerber, J.A.; Lu, Y.; Zeiher, J.; Stamper-Kurn, D.M. Superresolution microscopy of optical fields using tweezer-trapped single atoms. *Phys. Rev. Lett.* **2022**, *128*, 083201. [CrossRef] [PubMed]
25. Madjarov, I.S.; Cooper, A.; Shaw, A.L.; Covey, J.P.; Schkolnik, V.; Yoon, T.H.; Williams, J.R.; Endres, M. An atomic-array optical clock with single-atom readout. *Phys. Rev. X* **2019**, *9*, 041052. [CrossRef]
26. Schlosser, N.; Reymond, G.; Protsenko, I.; Grangier, P. Sub-poissonian loading of single atoms in a microscopic dipole trap. *Nature* **2001**, *411*, 1024–1027. [CrossRef]
27. Schlosser, N.; Reymond, G.; Grangier, P. Collisional blockade in microscopic optical dipole traps. *Phys. Rev. Lett.* **2002**, *89*, 023005. [CrossRef]
28. Sheng, C.; Hou, J.; He, X.; Xu, P.; Wang, K.; Zhuang, J.; Li, X.; Liu, M.; Wang, J.; Zhan, M. Efficient preparation of two-dimensional defect-free atom arrays with near-fewest sorting-atom moves. *Phys. Rev. Res.* **2016**, *3*, 023008. [CrossRef]
29. Schymik, K.-N.; Lienhard, V.; Barredo, D.; Scholl, P.; Williams, H.; Browaeys, A.; Lahaye, T. Enhanced atom-by-atom assembly of arbitrary tweezer arrays. *Phys. Rev. A* **2020**, *102*, 063107. [CrossRef]
30. Tian, W.; Wee, W.J.; Qu, A.; Lim, B.J.M.; Datla, P.R.; Koh, V.P.W.; Loh, H. Parallel assembly of arbitrary defect-free atom arrays with a multitweezer algorithm. *Phys. Rev. Appl.* **2023**, *19*, 034048. [CrossRef]
31. Zhou, Y.; Kanoda, K.; Ng, T.-K. Quantum spin liquid states. *Rev. Mod. Phys.* **2017**, *89*, 025003. [CrossRef]

32. Li, C.; Yang, S.; Xu, J. Quantum phases of Rydberg atoms on a frustrated triangular-lattice array. *Opt. Lett.* **2022**, *47*, 1093–1096. [CrossRef] [PubMed]
33. Samajdar, R.; Ho, W.; Pichler, H.; Lukin, M.; Sachdev, S. Quantum phases of Rydberg atoms on a kagome lattice. *Proc. Natl. Acad. Sci. USA* **2021**, *118*, e2015785118. [CrossRef]
34. Wurtz, J.; Bylinskii, A.; Braverman, B.; Amato-Grill, J.; Cantu, S.H.; Huber, F.; Lukin, A.; Liu, F.; Weinberg, P.; Long, J.; et al. Aquila: Quera's 256-qubit neutral-atom quantum computer. *arXiv* **2023**, arXiv:2306.11727.
35. Shen, H.Z.; Wang, Q.; Wang, J.; Yi, X.X. Nonreciprocal unconventional photon blockade in a driven dissipative cavity with parametric amplification. *Phys. Rev. A* **2020**, *101*, 013826.
36. Shen, H.Z.; Shang, C.; Zhou, Y.H.; Yi, X.X. Nonreciprocal Unconventional single-photon blockade in non-Markovian systems. *Phys. Rev. A* **2018**, *98*, 023856.
37. Zhang, J.T.; Picard, L.R.; Cairncross, W.B.; Wang, K.; Yu, Y.; Fang, F.; Ni, K.-K. An optical tweezer array of ground-state polar molecules. *Quantum Sci. Technol.* **2022**, *7*, 035006. [CrossRef]